

Carboxyl-Bonded Low-Spin Iron(III). Chemistry of a Family of Coordination Type *cis*-FeN₄O₂

Soma Karmakar and Animesh Chakravorty*

Department of Inorganic Chemistry, Indian Association for the Cultivation of Science, Calcutta 700 032, India

Received July 29, 1995[⊗]

Three tridentate ligands H₂PhL (Ar = Ph), H₂ToL (Ar = *p*-tolyl), and H₂NpL (Ar = α -naphthyl) of structural type HON=C(Ar)N=NC₆H₄CO₂H have been synthesized. These (general abbreviation H₂ArL) react with iron(III) chloride, affording the pink Et₄N[Fe(ArL)₂] ($s = 1/2$; $\mu_{\text{eff}} = 1.98\text{--}2.04 \mu_{\text{B}}$) in which azo oxime chelation ensures spin-pairing while carboxylate coordination stabilizes the trivalent state. The EPR spectra of the complexes in frozen dimethylformamide–toluene glass (77 K) are rhombic with *g* values in the range 1.997–2.173. The X-ray structure of Et₄N[Fe(NpL)₂]·H₂O·CH₂Cl₂ has been determined, revealing meridional binding of the two ligands affording *cis*-FeN₄O₂ geometry. The effect of spin-pairing is expressed in the relatively short (~1.90 Å) Fe–O and Fe–N lengths. The water of crystallization is hydrogen-bonded to carboxyl O atoms. The iron(III)–iron(II) reduction potentials lie near –0.1 V vs SCE. Crystal data for Et₄N[Fe(NpL)₂]·H₂O·CH₂Cl₂: crystal system triclinic, space group $P\bar{1}$, $a = 11.539(9) \text{ \AA}$, $b = 13.306(13) \text{ \AA}$, $c = 14.60(2) \text{ \AA}$, $\alpha = 89.30(9)^\circ$, $\beta = 82.65(9)^\circ$, $\gamma = 79.90(8)^\circ$, $V = 2189(4) \text{ \AA}^3$, $Z = 2$, $R = 6.59\%$, $R_w = 6.23\%$.

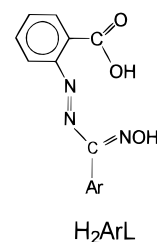
Introduction

Coordination by the carboxyl group is a pervasive feature of iron(III) chemistry and biochemistry.^{1–4} But for one exception,⁵ systems incorporating such binding are universally high-spin ($s = 5/2$ per iron(III)). Species of the low-spin ($s = 1/2$) category remain a synthetic and structural curiosity, and the prospect of realizing them aroused our interest. The ligation of less common 3d spin states has been a general concern of this laboratory.^{6–8}

Herein we report the design of a family of acyclic tridentate ligands that has afforded low-spin iron(III) complexes of coordination type *cis*-FeN₄O₂. Carboxyl binding is authenticated by X-ray structure determination. Magnetic, spectral, and redox behaviors of the complexes are scrutinized.

Results and Discussion

Ligands. The three ligands used are H₂PhL, H₂ToL, and H₂NpL, generally abbreviated as H₂ArL, **1**. These yellow solids incorporate carboxyl, azo, and oxime functions as potential



H₂ArL

1

Ar	H ₂ ArL
phenyl	H ₂ PhL
<i>p</i> -tolyl	H ₂ ToL
α -naphthyl	H ₂ NpL

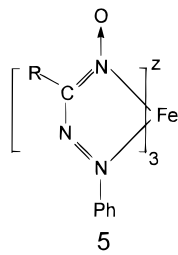
donor sites. The starting material for synthesis of H₂ArL (Scheme 1; structures **2–4**) is 2-aminobenzoic acid. The amino group is transformed into the azo oxime function by the reaction sequence of Scheme 1, the carboxyl group being preserved throughout.

The carboxyl function is a weaker-field ligand than water,⁹ and further the spin-pairing energy of the iron(III) (3d⁵) is especially high.¹⁰ To achieve low-spin configuration for iron(III) in an environment having carboxyl coordination, it is evidently necessary to have companion donor sites that strongly promote spin-pairing. The selection of azo oxime as the companion function was based on our experience with low-spin azo oxime tris chelates of type **5**. Here the iron(II) state (z

* Corresponding author. Telefax: +91-33-473-2805. email: icac@iacs.ernet.in.

- [⊗] Abstract published in *Advance ACS Abstracts*, February 1, 1996.
- (1) Que, L. Jr.; True, A. E. *Progr. Inorg. Chem.* **1990**, *38*, 97.
- (2) (a) Powell, A. K. *Coord. Chem. Rev.* **1994**, *134*, 130. (b) Ward, M. D. *Coord. Chem. Rev.* **1992**, *115*, 1.
- (3) Hartman, J. R.; Rardin, R. L.; Chaudhuri, P.; Pohl, K.; Wieghardt, K.; Nuber, B.; Weiss, J.; Papaefthymiou, G. C.; Frankel, R. B.; Lippard, S. J. *J. Am. Chem. Soc.* **1987**, *109*, 7387.
- (4) (a) Turowski, P. N.; Armstrong, W. H.; Liu, S.; Brown, S. N.; Lippard, S. J. *Inorg. Chem.* **1994**, *33*, 636. (b) Taft, K. L.; Papaefthymiou, G. C.; Lippard, S. J. *Inorg. Chem.* **1994**, *33*, 1510.
- (5) Curtis, N. F.; Xin, L.; Weatherburn, D. C. *Inorg. Chem.* **1993**, *32*, 5838.
- (6) Karmakar, S.; Choudhury, S. B.; Chakravorty, A. *Inorg. Chem.* **1994**, *33*, 6148.
- (7) (a) Basu, P.; Pal, S.; Chakravorty, A. *Inorg. Chem.* **1988**, *27*, 1848. (b) Chattopadhyay, S.; Basu, P.; Pal, S.; Chakravorty, A. *J. Chem. Soc., Dalton Trans.* **1990**, 3829.
- (8) (a) Basu, P.; Choudhury, S. B.; Pal, S.; Chakravorty, A. *Inorg. Chem.* **1989**, *28*, 2680. (b) Basu, P.; Chakravorty, A. *Inorg. Chem.* **1992**, *31*, 4980. (c) Basu, P.; Chakravorty, A. *J. Chem. Soc., Chem. Commun.* **1992**, 809.

- (9) Lever, A. B. P. *Inorganic Electronic Spectroscopy*, 2nd ed.; Elsevier: New York, 1984; p 750.
- (10) Cotton, F. A.; Wilkinson, G. *Advanced Inorganic Chemistry: A Comprehensive Text*, 4th ed.; Wiley-Interscience: New York, 1980; p 644.



$= -1$) is stable, but the iron(III) state ($z = 0$) is not.¹¹ We guessed that insertion of a carboxyl substituent in the azo oxime Ph group might afford a ligand with the desired iron(III) binding properties.

Low-Spin Iron(III) Complexes. The reaction of anhydrous iron(III) chloride and H_2ArL in 1:2 ratio in methanol containing Et_4NCl afforded a pink salt of composition $Et_4N[Fe(ArL)_2]$ in excellent yields. Single crystals of the NpL^{2-} complex could however be grown only in a solvated form; *vide infra*.

Selected characterization data are listed in Table 1. The 1:1 electrolytic complexes display characteristic absorption spectra in the visible region (Table 1; Figure 1). The bands are believed to be of $\pi(ArL^{2-}) \rightarrow d(Fe)$ origin.

The room-temperature magnetic moments of $Et_4N[Fe(ArL)_2]$ lie close to $2.0 \mu_B$ (Table 2), corresponding to the t_2^5 configuration with incomplete quenching of orbital moment. The variable-temperature moment of $Et_4N[Fe(PhL)_2]$ (Figure 2) reveals the expected slight decrease with temperature.¹²

In frozen dimethylformamide–toluene (1:1) glass (77 K), $Et_4N[Fe(ArL)_2]$ displays well-resolved rhombic EPR spectra (Table 2, Figure 2), consistent with the *cis*- FeN_4O_2 coordination sphere revealed by structure determination (see below). This geometry can at best have a 2-fold axis and is therefore inherently rhombic.

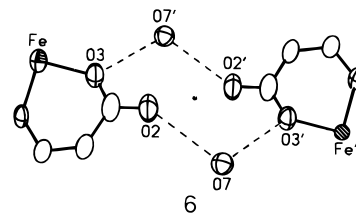
Crystal and Molecular Structure. Only the NpL^{2-} complex afforded good single crystals in the form of the solvate $Et_4N[Fe(NpL)_2] \cdot H_2O \cdot CH_2Cl_2$. A view of the $Fe(NpL)_2^-$ ion is shown in Figure 3, and selected bond parameters are listed in Table 3. The CH_2Cl_2 molecule and the Et_4N^+ cations occur as discrete entities in the lattice without any unusual nonbonded contacts with other atoms. The water molecule is hydrogen-bonded to the complex anion (see below).

The two ligands span meridionally, binding the metal in the hexadentate FeN_4O_2 fashion utilizing pairs of oximate N, azo N, and carboxyl O atoms, resulting in *cis* configuration for the FeN_4O_2 coordination sphere. Distortions from the idealized octahedral geometry are large. The angles at the metal center between *cis*-positioned donor pairs span the range $79.1(3) - 99.5(3)^\circ$, and those between *trans*-positioned pairs are $165.9(3) - 178.5(3)^\circ$.

The two tridentate ligands have the same gross structure but with some subtle conformational differences. The ligands incorporating N1 and N4 will be respectively identified as A and B. For both, the five-membered azo-oxime chelate ring including the pendant oximate O atom is an excellent plane with mean deviation of $\sim 0.02 \text{ \AA}$. The naphthyl plane is inclined to it by 59.0° in **A** and by 51.2° in **B**. The six-membered chelate rings deviate significantly from planarity (mean deviation $\sim 0.1 \text{ \AA}$). The benzene ring bearing the carboxyl function is rotated

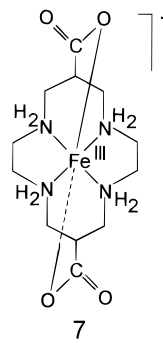
around the C–N bond away from the azo-oxime chelate ring by 12.2° in **A** and 18.3° in **B**. The carboxyl function is nearly coplanar with the benzene ring in **A**, but in **B** it forms a dihedral angle of 15.4° .

The carboxyl function of chelate **A** alone is involved in hydrogen-bonding with the water of crystallization. The uncoordinated atom, O2, has an $O2 \cdots O7$ contact of length $2.952(11) \text{ \AA}$. The water molecule forms a second slightly longer ($O7 \cdots O3'$, $3.030(11) \text{ \AA}$) hydrogen bond with the coordinated carboxyl oxygen, $O3'$, of an adjacent complex ion. The $O2 \cdots O7 \cdots O3'$ angle is 105.4° . In effect, the lattice consists of centrosymmetric water-bridged dimers, as shown in the structure fragment **6**. The coordinates of primed and unprimed atoms in **6** are \bar{x} , $1 - y$, \bar{z} and x , y , z , respectively.



The four Fe–N lengths are virtually the same within experimental error, the average value being $1.897(6) \text{ \AA}$. On the other hand, the Fe– $O3$ length, $1.919(6) \text{ \AA}$, is $\sim 0.04 \text{ \AA}$ longer than the Fe– $O6$ length, $1.879(6) \text{ \AA}$. Significantly, the $O3$ atom is involved in hydrogen-bonding as in **6**, but $O6$ is not. Spin-pairing leads to an effective decrease in metal radius.¹³ For high-spin iron(III) complexes, the expected Fe–N (sp^2 hybridized) and Fe–O (carboxylate) lengths are ~ 2.1 and $\sim 2.0 \text{ \AA}$, respectively.¹⁴ The lengths in $Fe(NpL)_2^-$ are shorter than these values by nearly 0.2 and 0.1 \AA , respectively.

The only known low-spin iron(III)–carboxylate complex is macrocycle **7**, in which the FeN_4O_2 coordination sphere has *trans*



configuration.⁵ The average Fe–N and Fe–O lengths are $1.994(3)$ and $1.895(2) \text{ \AA}$, respectively, the N atoms being sp^3 hybridized unlike those in our complex (sp^2). The shorter (by $\sim 0.1 \text{ \AA}$) average Fe–N length observed in $Fe(NpL)_2^-$ is consistent with this change in nitrogen hybridization. The average Fe–O distances in **7** and $Fe(NpL)_2^-$ are nearly equal. In $Fe(ArL)_2^-$, we now have the first family of low-spin iron(III) carboxylates derived from acyclic ligands.

Metal Redox. In dimethylformamide solution (0.1 M TEAP) the $Et_4N[Fe(ArL)_2]$ complexes display a cyclic one-electron response near -0.06 V vs SCE. Reduction potential and coulometric data are collected in Table 1. Exhaustive reduction at -0.3 V leads to one-electron transfer affording a green solution which has the same voltammogram (initial scan anodic)

(11) (a) Pal, S.; Melton, T.; Mukherjee, R. N.; Chakravarty, A. R.; Tomas, M.; Falvello, L. R.; Chakravorty, A. *Inorg. Chem.* **1985**, *24*, 1250. (b) Pal, S.; Mukherjee, R. N.; Tomas, M.; Falvello, L. R.; Chakravorty, A. *Inorg. Chem.* **1986**, *25*, 200. (c) Manivannan, V.; Chattopadhyay, S.; Basu, P.; Chakravorty, A. *Polyhedron* **1993**, *12*, 2725.
(12) (a) Figgis, B. N. *Trans. Faraday Soc.* **1961**, *57*, 198. (b) *Ibid.* **1961**, *57*, 204.

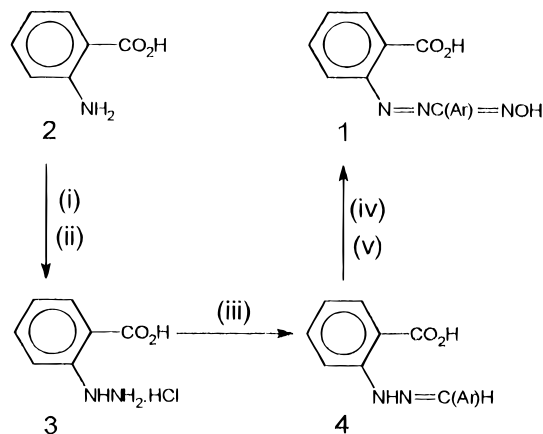
(13) (a) Shannon, R. D. *Acta Crystallogr.* **1976**, *A32*, 751. (b) Shannon, R. D.; Prewitt, C. T. *Acta Crystallogr.* **1969**, *B25*, 925.

(14) Lin, W.; Welsh, W. J.; Harris, W. R. *Inorg. Chem.* **1994**, *33*, 884.

Table 1. Conductivity, Electrochemical,^a and Electronic Spectral Data in Dimethylformamide at 298 K

compd	Λ , $\Omega^{-1} \text{ cm}^2 \text{ M}^{-1}$	$E_{1/2}^{b,c}$ V (ΔE_p^c , mV); $n^{c,d}$	UV-vis data: λ_{max} , nm (ϵ , $\text{M}^{-1} \text{ cm}^{-1}$)
$\text{Et}_4\text{N}[\text{Fe}(\text{PhL})_2]$	74	-0.05 (70); 0.99	925 (920), 600 ^f (5680), 520 (14 130)
$\text{Et}_4\text{N}[\text{Fe}(\text{NpL})_2]$	69	-0.08 (80); 1.01	925 (930), 600 ^f (5900), 500 (15 560)
$\text{Et}_4\text{N}[\text{Fe}(\text{ToL})_2]$	70	-0.06 (80); 1.02	925 (916), 600 ^f (5220), 500 (12 440)

^a At a platinum disk electrode; supporting electrolyte tetraethylammonium perchlorate (TEAP, 0.1 M); scan rate 50 mV s^{-1} ; reference electrode SCE; solute concentration $\sim 10^{-3}$ M. ^b $E_{1/2}$ is calculated as the average of anodic (E_{pa}) and cathodic (E_{pc}) peak potentials. ^c $\Delta E_p = E_{pa} - E_{pc}$. ^d $n = Q/Q'$, where Q is the observed Coulomb count and Q' is the calculated count for 1e transfer. ^e Constant-potential electrolysis performed at 200 mV below E_{pc} for reduction and 200 mV above E_{pa} for oxidation. ^f Shoulder.

Scheme 1^a

^a (i) Concentrated HCl, NaNO_2 , 0 °C. (ii) SnCl_2 , 0 °C. (iii) NaOAc, HOAc, ArCHO, 25 °C. (iv) *n*-BuNO₂, NaOMe, MeOH, reflux. (v) Dilute NaOH, extract with Et₂O, neutralize aqueous part with dilute H₂SO₄, 0 °C.

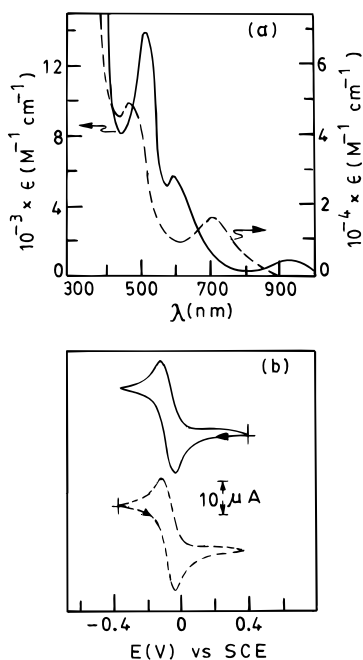
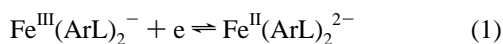


Figure 1. (a) Electronic spectra of $\text{Et}_4\text{N}[\text{Fe}(\text{PhL})_2]$ (—) and electrogenerated $\text{Fe}(\text{PhL})_2^{2-}$ (---) in dimethylformamide. (b) Cyclic voltammograms (scan rate 50 mV s^{-1}) of 10^{-3} M solutions of $\text{Et}_4\text{N}[\text{Fe}(\text{PhL})_2]$ (—) and electrogenerated $\text{Fe}(\text{PhL})_2^{2-}$ (---) in dimethylformamide (0.1 M TEAP) at 298 K at platinum electrode.

as the parent $\text{Fe}(\text{ArL})_2^-$ complex (initial scan cathodic). We thus have the couple of eq 1. The two species are believed to



have the same gross structure, since the redox response is nearly reversible.

Table 2. Magnetic Moments^a and EPR Data^b

compd	μ_{eff} , μ_B	g values		
		g_1	g_2	g_3
$\text{Et}_4\text{N}[\text{Fe}(\text{PhL})_2]$	2.01	2.173	2.127	1.997
$\text{Et}_4\text{N}[\text{Fe}(\text{NpL})_2]$	1.98	2.173	2.121	1.997
$\text{Et}_4\text{N}[\text{Fe}(\text{ToL})_2]$	2.04	2.173	2.124	1.998

^a In the solid state at 298 K. ^b Frozen dimethylformamide–toluene (1:1) glass at 77 K.

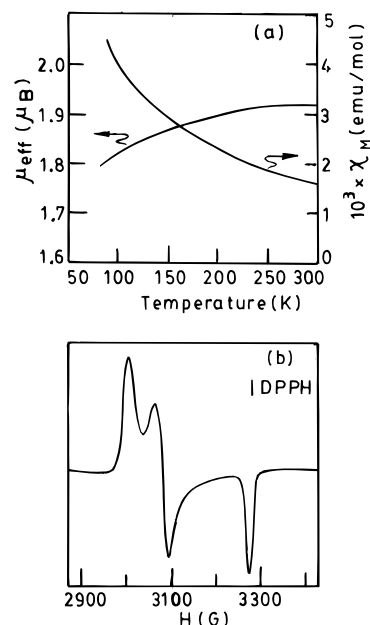


Figure 2. (a) Plots of the magnetic moment μ_{eff} (μ_B) and the magnetic susceptibility χ_M (emu/mol) against temperature T (K) for $\text{Et}_4\text{N}[\text{Fe}(\text{PhL})_2]$. (b) X-band EPR spectrum of $\text{Et}_4\text{N}[\text{Fe}(\text{NpL})_2]$ in frozen 1:1 dimethylformamide–toluene solution at 77 K.

Electrogenerated solutions of $\text{Fe}(\text{ArL})_2^{2-}$ are EPR-inactive consistent, with either low-spin ($s = 0$) or high-spin ($s = 2$, EPR-silent) states. In general, ligands which promote spin-pairing in iron(III) do so in iron(II) also.^{6,8,11c} This happens because the drastically reduced (between iron(III) and iron(II)) spin-pairing energy is still more than balanced by the crystal field stabilization even though it is also sizably reduced.^{9,10} On this count, the $\text{Fe}(\text{RL})_2^{2-}$ species are believed to be low-spin. A representative electronic spectrum of the reduced complex is shown in Figure 1. The bands at 710 and 475 nm are tentatively assigned to $d(\text{Fe}) \rightarrow \pi^*(\text{ArL}^{2-})$ excitation. Because of the low $E_{1/2}$ value of the couple of eq 1, $\text{Fe}^{\text{II}}(\text{ArL})_2^{2-}$ solutions are spontaneously oxidized by air to $\text{Fe}^{\text{III}}(\text{ArL})_2^-$.

It is instructive to compare $\text{Fe}(\text{ArL})_2^-$ with the tris chelate **5**. In the latter, the iron(III)–iron(II) $E_{1/2}$ is only moderately high, ~ 0.3 V, but even then, the iron(III) species are unstable.¹¹ The azo–oxime function is essentially a soft and strong-field ligand with superior iron(II) affinity. On the other hand, carboxyl oxygen is a hard donor, binding iron(III) well. In $\text{Fe}(\text{ArL})_2^-$, azo–oxime chelation ensures spin-pairing while

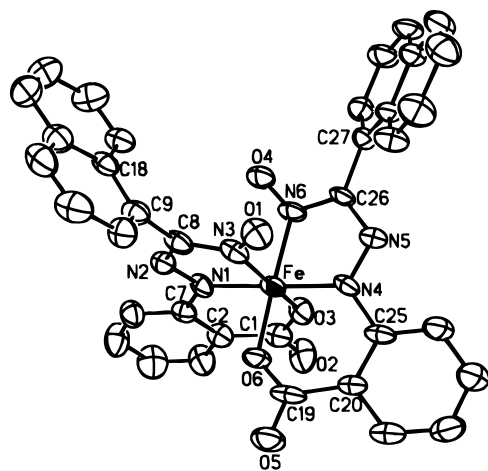


Figure 3. ORTEP plot and atom-labeling scheme for $\text{Et}_4\text{N}[\text{Fe}(\text{NpL})_2]$. All atoms are represented by their 50% thermal probability ellipsoids.

Table 3. Selected Bond Distances (Å) and Angles (deg) and Their Estimated Standard Deviations for $\text{Et}_4\text{N}[\text{Fe}(\text{NpL})_2] \cdot \text{H}_2\text{O} \cdot \text{CH}_2\text{Cl}_2$

Distances			
Fe–N1	1.892(6)	O2–C1	1.232(10)
Fe–N3	1.907(6)	O3–C1	1.285(11)
Fe–N4	1.888(6)	O5–C19	1.219(10)
Fe–N6	1.899(7)	O6–C19	1.263(8)
Fe–O3	1.919(6)	O1–N3	1.249(8)
Fe–O6	1.879(6)	O4–N6	1.257(8)
N1–N2	1.299(8)	O2...O7	2.952(11)
N4–N5	1.287(9)	O7...O3'	3.030(11) ^a
Angles			
N1–Fe–N3	81.1(3)	O3–Fe–N4	88.1(2)
N1–Fe–N4	178.5(3)	O3–Fe–N6	95.0(3)
N1–Fe–N6	99.5(3)	O3–Fe–O6	96.8(2)
N3–Fe–N4	98.5(3)	O6–Fe–N1	87.9(2)
N3–Fe–N6	80.0(3)	O6–Fe–N3	89.4(3)
N4–Fe–N6	79.1(3)	O6–Fe–N4	93.5(2)
O3–Fe–N1	92.1(2)	O6–Fe–N6	165.9(3)
O3–Fe–N3	170.7(2)	O2...O7...O3'	105.4(3) ^a

^a Coordinates of primed atom: $\bar{x}, 1 - y, \bar{z}$.

carboxylate coordination stabilizes the trivalent state, also lowering the iron(III)–iron(II) reduction potential.

Concluding Remarks. The main findings of this work will now be summarized. The oxime–azo–carboxylate ligand system, H_2ArL , has been designed, affording low-spin carboxyl-bonded iron(III) salts of the type $\text{Et}_4\text{N}[\text{Fe}(\text{ArL})_2]$ in which the metal coordination geometry is *cis*- FeN_4O_2 . Upon collective consideration of stabilities and reduction potentials of $\text{Fe}(\text{ArL})_2^-$ and the tris chelate **5**, it is proposed that in the former azo–oxime chelation ensures spin-pairing while carboxylate coordination stabilizes the trivalent state. The Fe–N and Fe–O lengths in $\text{Fe}(\text{NpL})_2^-$ are significantly shorter (by 0.1–0.2 Å) than those in representative high-spin species.

Prior to this work, only one low-spin carboxyl-bonded iron(III) complex of a macrocyclic ligand had been documented (*trans*- FeN_4O_2 coordination). The present complexes are the first species incorporating an acyclic ligand system (*cis*- FeN_4O_2 coordination). With judicious choice of coligand functions, it should in principle be possible to tailor new ligands that could stabilize the difficultly achievable low-spin state of iron(III) in a carboxyl-coordinated environment.

Experimental Section

Physical Measurements. A Hitachi 330 spectrophotometer was used to record UV–vis spectra. EPR spectra were studied with a Varian E-109C spectrometer fitted with a quartz dewar. Magnetic susceptibilities were measured with a Model 155 PAR vibrating-sample mag-

netometer fitted with a Walker Scientific L75FBAL magnet and a Model 153N dewar along with a temperature controller. A Perkin-Elmer 240C elemental analyzer was used to collect microanalytical data (CHN). Electrochemical measurements were performed under nitrogen atmosphere on a PAR 370-4 electrochemistry system using solvents and supporting electrolyte purified/prepared as before.^{8a,15} Solution electrical conductivities were measured with the help of a Philips PR 9500 bridge, the solute concentration being $\sim 10^{-3}$ M.

Synthesis of Ligands and Complexes. The ligands were prepared by the same general procedure outlined in Scheme 1, and complexes were also synthesized by a general method. Details are given below for H_2NpL and its iron(III) complex. The solvents and chemicals used for synthesis were of analytical grade.

2-(Carboxyphenyl)hydrazine Hydrochloride, 3. A solution of sodium nitrite (2.50 g, 0.036 mol) in 5 mL water was added slowly to a suspension of *o*-aminobenzoic acid, **2** (2.74 g, 0.020 mol), in 10 mL of concentrated HCl at 0 °C, affording a clear greenish yellow solution, which was left at 0 °C for a further period of 0.25 h. A cold solution (0 °C) of stannous chloride (12 g, 0.053 mol) in 10 mL of concentrated HCl was then added with vigorous stirring which was continued for 1.5 h. The white precipitate that separated from the mixture was collected by filtration and dissolved in 20 mL of water to obtain a clear and transparent solution, and then 150 mL of concentrated HCl was added to it with constant stirring. The hydrazine hydrochloride, **3**, started precipitating immediately, and the mixture was cooled overnight in a refrigerator. The silky white solid was collected by filtration and was used without further purification in the next step. Yield: 3.0 g (79%).

Naphthaldehyde 2-(Carboxyphenyl)hydrazone, 4. A 3.0 g (0.016 mol) sample of **3** was dissolved in 15 mL of water containing sodium acetate trihydrate (4.53 g, 0.033 mol) and glacial acetic acid (10–15 mL). The solution was filtered to remove insoluble material, if present. To this was added slowly naphthaldehyde (2.49 g, 0.016 mol) with vigorous stirring which was continued for 2 h. The pale yellow hydrazone appeared immediately. It was collected by filtration washed thoroughly with water, and then dried in vacuo over fused CaCl_2 to obtain the required hydrazone, as a pale yellow solid. Yield: 3.5 g (76%). Anal. Calcd for $\text{C}_{18}\text{H}_{14}\text{N}_2\text{O}_2$: C, 74.48; H, 4.83; N, 9.65. Found: C, 74.55; H, 4.80; N, 9.69. Mp: 208–210 °C.

Anal. Calcd for **4** (Ar = Ph), $\text{C}_{14}\text{H}_{12}\text{N}_2\text{O}_2$: C, 70.00; H, 5.00; N, 11.67. Found: C, 70.08; H, 4.90; N, 11.62. Mp: 203–205 °C. Anal. Calcd for **4** (Ar = To), $\text{C}_{15}\text{H}_{14}\text{N}_2\text{O}_2$: C, 70.87; H, 5.51; N, 11.02. Found: C, 70.75; H, 5.60; N, 11.15. Mp: 200–203 °C.

((2-Carboxyphenyl)azo)-1-naphthaldoxime, 1. A 3.5 g (0.012 mol) sample of **4** was suspended in 25 mL of dry methanol, and 10 mL of freshly prepared *n*- BuNO_2 was added to the suspension, followed by a solution of NaOMe in methanol (prepared from 0.70 g of Na in 20 mL of hot methanol). The blood red mixture was stirred and then heated to reflux for 1 h. It was then cooled, and an ice-cold solution of 1.20 g of NaOH in 20 mL water was added slowly. The mixture was allowed to stand for 12 h at room temperature and then extracted with diethyl ether. The aqueous layer was cooled in ice and then neutralized slowly with cold 1 N H_2SO_4 until it became just acidic. During this process, the color of the solution became progressively lighter and finally the ligand, **1**, separated out as a crystalline yellow solid which was collected by filtration. It was washed several times with water and finally dried in vacuo over fused CaCl_2 . Yield: 3.2 g (83%). Anal. Calcd for **1**, $\text{C}_{18}\text{H}_{13}\text{N}_3\text{O}_3$: C, 67.71; H, 4.07; N, 13.16. Found: C, 67.65; H, 4.12; N, 13.08. Mp: 150–152 °C. λ_{max} , nm (ϵ , $\text{cm}^{-1} \text{M}^{-1}$): 360 (5680), 330 (6290).

Anal. Calcd for **1** (Ar = Ph), $\text{C}_{14}\text{H}_{11}\text{N}_3\text{O}_3$: C, 62.45; H, 4.09; N, 15.61. Found: C, 62.54; H, 4.21; N, 15.52. Mp: 145–147 °C. λ_{max} , nm (ϵ , $\text{cm}^{-1} \text{M}^{-1}$): 360 (5790), 330 (6230). Anal. Calcd for **1** (Ar = To), $\text{C}_{15}\text{H}_{13}\text{N}_3\text{O}_3$: C, 63.60; H, 4.59; N, 14.84. Found: C, 63.71; H, 4.52; N, 14.95. Mp: 142–144 °C. λ_{max} , nm (ϵ , $\text{cm}^{-1} \text{M}^{-1}$): 360 (5780), 330 (6360).

Tetraethylammonium Bis(((2-carboxylatophenyl)azo)-1-naphthaldoximate)ferrate(III), $\text{Et}_4\text{N}[\text{Fe}(\text{NpL})_2]$. The complex was prepared by adding a methanolic solution (10 mL) of H_2NpL (0.39 g, 1.22

Table 4. Crystallographic Data for $\text{Et}_4\text{N}[\text{Fe}(\text{NpL})_2] \cdot \text{H}_2\text{O} \cdot \text{CH}_2\text{Cl}_2$

empirical formula	$\text{C}_{45}\text{H}_{46}\text{Cl}_2\text{N}_7\text{O}_7\text{Fe}$	Z	2
fw	923.6	$T, ^\circ\text{C}$	22
space group	$P\bar{1}$	$\lambda, \text{\AA}$	0.710 73
$a, \text{\AA}$	11.539(9)	$\rho_{\text{calcd}}, \text{g cm}^{-3}$	1.401
$b, \text{\AA}$	13.306(13)	μ, cm^{-1}	5.26
$c, \text{\AA}$	14.60(2)	transm coeff	0.75–0.85
α, deg	89.30(9)	R^a	6.59
β, deg	82.65(9)	R_w^b	6.23
γ, deg	79.90(8)	GOF ^c	1.20
$V, \text{\AA}^3$	2189(4)		

^a $R = \sum ||F_o| - |F_c|| / \sum |F_o|$. ^b $R_w = [\sum w(|F_o| - |F_c|)^2 / \sum w|F_o|^2]^{1/2}$; $w^{-1} = \sigma^2(|F_o|) + g|F_o|^2$; $g = 0.000$ for $\text{Et}_4\text{N}[\text{Fe}(\text{NpL})_2] \cdot \text{H}_2\text{O} \cdot \text{CH}_2\text{Cl}_2$.

^c The goodness of fit is defined as $[w(|F_o| - |F_c|)^2 / (n_o - n_v)]^{1/2}$, where n_o and n_v denote the numbers of data and variables, respectively.

mmol) containing Et_4NCl (0.12 g, 0.650 mmol) to a solution containing anhydrous ferric chloride (0.10 g, 0.620 mol). A pink color developed, and it darkened quickly. The mixture was stirred at room temperature for 1 h. The deposited dark crystalline solid was filtered off, washed several times with aqueous methanol (1:1), and dried in vacuo over CaCl_2 . Yield: 0.38 g (76%). Anal. Calcd for $\text{Et}_4\text{N}[\text{Fe}(\text{NpL})_2] \cdot \text{C}_{44}\text{H}_{42}\text{N}_7\text{O}_6\text{Fe}$: C, 64.43; H, 5.13; N, 11.96. Found: C, 64.50; H, 5.03; N, 11.92.

Anal. Calcd for $\text{Et}_4\text{N}[\text{Fe}(\text{PhL})_2] \cdot \text{C}_{36}\text{H}_{38}\text{N}_7\text{O}_6\text{Fe}$: C, 60.04; H, 5.28; N, 13.62. Found: C, 60.10; H, 5.15; N, 13.71. Anal. Calcd for $\text{Et}_4\text{N}[\text{Fe}(\text{ToL})_2] \cdot \text{C}_{38}\text{H}_{42}\text{N}_7\text{O}_6\text{Fe}$: C, 61.00; H, 5.62; N, 13.11. Found: C, 61.14; H, 5.74; N, 13.01.

X-ray Structure Determination. Crystals of $\text{Et}_4\text{N}[\text{Fe}(\text{NpL})_2] \cdot \text{H}_2\text{O} \cdot \text{CH}_2\text{Cl}_2$ ($0.38 \times 0.24 \times 0.40 \text{ mm}^3$) were grown by slow diffusion of hexane into wet dichloromethane solution followed by slow evaporation. The unit cell parameters were determined by the least-squares fit of 30 machine-centered reflections having 2θ values in the range 15–25°. Data were collected at 296 K by the ω -scan method over a 2θ range of 3–45° on a Nicolet R3m/V diffractometer with graphite-monochromated Mo $K\alpha$ radiation ($\lambda = 0.710 73 \text{ \AA}$). Two check reflections measured after every 98 reflections showed no significant intensity reduction during 50.45 h of exposure to X-rays. Lorentz and polarization corrections as well as a semiempirical absorption correction¹⁶ were made. The structure was successfully solved in space group $P\bar{1}$. Of the 5732 unique reflections, 3403 satisfying $I > 2.5\sigma(I)$ were used for structure solution. The structure was solved by direct methods and was refined by full-matrix least-squares procedures, making all non-hydrogen atoms anisotropic. Hydrogen atoms were included in calculated positions with fixed U ($=0.08 \text{ \AA}^2$). The highest residual was 0.68 e \AA^{-3} . Significant crystal data are listed in Table 4. Essential atomic coordinates and isotropic

Table 5. Essential Atomic Coordinates ($\times 10^4$) and Equivalent^a Isotropic Displacement Coefficients ($\text{\AA}^2 \times 10^3$) for $\text{Et}_4\text{N}[\text{Fe}(\text{NpL})_2] \cdot \text{H}_2\text{O} \cdot \text{CH}_2\text{Cl}_2$

	x	y	z	$U(\text{eq})$
Fe	285(1)	2090(1)	2416(1)	40(1)
O1	-299(5)	543(4)	3645(4)	61(2)
O2	868(5)	4459(4)	799(4)	77(3)
O3	236(5)	3192(4)	1554(3)	52(2)
O4	236(5)	545(4)	1134(3)	58(2)
O5	517(5)	3667(4)	4653(3)	68(2)
O6	724(5)	2786(3)	3392(3)	52(2)
N1	1920(5)	1622(4)	2036(3)	40(2)
N2	2360(5)	748(4)	2368(4)	43(2)
N3	487(6)	863(4)	3111(4)	45(2)
N4	-1354(5)	2531(4)	2775(4)	42(2)
N5	-2095(5)	2062(4)	2441(4)	45(2)
N6	-366(6)	1231(5)	1669(4)	46(2)
C1	1086(8)	3630(6)	1184(5)	56(4)
C2	2366(7)	3112(5)	1168(5)	49(3)
C7	2757(7)	2161(5)	1542(4)	42(3)
C8	1600(7)	311(5)	2942(5)	48(3)
C19	95(8)	3385(5)	3998(5)	52(3)
C20	-1191(7)	3789(5)	3904(5)	42(3)
C25	-1883(8)	3398(5)	3348(5)	47(3)
C26	-1567(6)	1322(5)	1848(5)	43(3)
O7	1835(7)	5852(6)	-565(5)	110(3)

^a Equivalent isotropic U defined as one-third of the trace of the orthogonalized U_{ij} tensor.

thermal parameters are collected in Table 5. Computations were carried out on a Micro VAX II computer using the SHELXTL-PLUS program system,¹⁷ and crystal structure plots were drawn using ORTEP.¹⁸

Acknowledgment. Financial support received from the Department of Science and Technology, New Delhi, is acknowledged. Affiliation with the Jawaharlal Nehru Centre for Advanced Scientific Research, Bangalore, India, is also acknowledged.

Supporting Information Available: Complete atomic coordinates (Table S1), bond distances (Table S2) and angles (Table S3), anisotropic thermal parameters (Table S4), and hydrogen atom positional parameters (Table S5) for $\text{Et}_4\text{N}[\text{Fe}(\text{NpL})_2] \cdot \text{H}_2\text{O} \cdot \text{CH}_2\text{Cl}_2$ (9 pages). Ordering information is given on any current masthead page.

IC950976Q

(16) North, A. C. T.; Philips, D. C.; Mathews, F. S. *Acta Crystallogr.* **1968**, A24, 351.

(17) Sheldrick, G. M. SHELXTL-PLUS 88. In *Structure Determination Software Programs*; Nicolet Instrument Corp.: 5225-2 Verona Rd, Madison, WI 53711, 1988.

(18) Johnson, C. K. ORTEP. Report ORNL-5138; Oak Ridge National Laboratory: Oak Ridge, TN, 1976.